Drug Delivery and Translational Research
https://doi.org/10.1007/s13346-024-01581-2

ORIGINAL ARTICLE

Resveratrol nanocrystals based dissolving microneedles with highly efficient for rheumatoid arthritis

Ningning Diao[1] · Yan Liu[2] · Wenxin Wang[1] · Min Cao[1] · Xiaowei Liu[1] · Weili Yang[1] · Yuxin Cao[1] · Tianying Sun[1] · Huijie Pei[1] · Chunjing Guo[3] · Daquan Chen[1]

Accepted: 16 March 2024

Abstract
Rheumatoid arthritis (RA) is a common immune disease characterized mainly by erosive arthritis with extensive clinical sequelae. Resveratrol (Res) has pharmacological effects in the treatment of RA, but it has not been widely used in the clinic due to its poor water solubility and low bioavailability. In this study, a drug delivery system (Res-NC MNs) of dissolved microneedles (MNs) loaded with Res nanocrystals (NC) was designed for the treatment of RA. Res-NC MNs can improve the drawbacks of long-term oral drug delivery with toxic side effects and low compliance associated with intra-articular drug delivery. In this study, Res-NC was prepared by media milling and loaded into soluble microneedles prepared from hyaluronic acid (HA) by vacuum casting for the treatment of RA. HA has high mechanical strength and can penetrate the cuticle layer of the skin for effective drug delivery. In in vivo pharmacodynamic experiments, Res-NC MNs achieved better therapeutic efficacy in the treatment of RA compared with oral Res. These findings suggest that Res-NC MNs may be an effective and promising drug delivery strategy for the treatment of RA.

Keywords Dissolvable microneedles · Nanocrystals · Resveratrol · Rheumatoid arthritis

Introduction

Rheumatoid arthritis (RA) is a chronic immune disease [1]. The progression of the disease may lead to structural destruction, deformity and even loss of function of the joints, eventually involving the skin, eyes, kidneys, lungs and other major organs, and it is one of the main diseases causing loss of labor and disability [2, 3]. Inflammation and immunological reactivity are predominantly restricted to the synovium, causing pain and articular injury, but are also linked to a slew of other complications [4, 5]. Currently, the main drugs used for anti-RA are non-steroidal anti-inflammatory drugs (NSAIDs) and corticosteroids, which are mainly administered orally and by intra-articular injection. Long-term oral administration is usually associated with first-pass effects and gastrointestinal side effects. Intra-articular injections are inconvenient because of pain, infection, high professionalism and lack of patient compliance [6–8]. Therefore, there is an urgent need to develop a novel mode of drug delivery for the treatment of RA, and the emergence of transdermal drug delivery systems has brought new hope to researchers.

Transdermal drug delivery system is a mode of drug delivery that can avoid oral and intra-articular injections as well as improve patients compliance. However, the existence of the stratum corneum poses an obstacle to transdermal drug delivery systems, and how to improve the delivery efficiency of transdermal drug delivery has become a new challenge [9, 10]. Microneedles (MNs), which are micrometer-sized needle-like devices with a needle body length of 20-2000 μm, are a mode of transdermal drug delivery [11]. The drug is encapsulated in

✉ Chunjing Guo
gcjgroup@126.com

✉ Daquan Chen
cdq1981@126.com

[1] Collaborative Innovation Center of Advanced Drug Delivery System and Biotech Drugs, School of Pharmacy, Yantai University, Yantai 264005, PR China

[2] Yantai Food and Drug Inspection and Testing Center, Yantai 264035, PR China

[3] College of Marine Life Science, Ocean University of China, Yushan 10 Road, Qingdao 266003, PR China

the tip of the MNs, which pierces the cuticle of the skin to form a channel that is absorbed by the capillaries and enters the blood circulation, thus realizing local or systemic drug delivery [12, 13]. MNs-mediated transdermal drug delivery can avoid the digestive and absorptive effects of the gastrointestinal tract, while avoiding the first-pass effect of the liver, thus improving bioavailability [14]. Also, because of the fine tip of the MNs, it can reduce the pain and achieve the effect of painless drug delivery, which improves the compliance of the patients [15, 16].

Resveratrol (Res) a polyphenolic compound widely found in plants such as grapes, thuja, and peanuts, is well known for its therapeutic benefits in the treatment of a variety of chronic diseases, including antioxidant, anti-viral, anti-fungal, cardioprotective, and anti-cancer and anti-inflammatory activities [17, 18]. In recent years, scientific studies have demonstrated that Res has a role in promoting the proliferation of osteoblasts, which has a non-negligible role in the treatment of rheumatoid arthritis [19]. However, its drawbacks such as poor water solubility and low bioavailability have severely limited its clinical application. Solubilizer, co-solvent, milling method and solid dispersion method are the main ways to improve the solubility. The advantages of preparing hydrophobic drugs into nanocrystals have received widespread attention [20].

Nanocrystals (NC) are colloidal dispersion systems in which the drug reaches a stable state of dispersion under the action of a small amount of stabilizer, and their size is generally in the range of 10 ~ 1000 nm, and the drug content is close to 100% [21, 22]. NC can increase the solubility of insoluble drugs by reducing the particle size of drug particles and increasing the specific surface area of drug particles [23, 24]. Therefore, conversion of Res into NC can significantly increase the solubility of Res. Therefore, by combining the advantages of both NC and MNs, it is believed that it can play a better role in the treatment of RA.

In this study, we designed for the first time a transdermal drug delivery system utilizing Res-NC-loaded MNs for the treatment of RA. The drawbacks associated with oral and articular delivery can be addressed by MNs, and in addition, carrier-free NC can increase the drug loading capacity of MNs while significantly improving the solubility of Res. We prepared Res as Res-NC by media milling method and loaded it into MNs prepared by vacuum casting method for the treatment of RA. It was found that Res-NC MNs alleviated the inflammatory effects and inhibited the progression of RA by suppressing excessive reactive oxygen species (ROS) during RA development. This study provides a novel strategy for the treatment of RA.

Materials and methods

Materials

Resveratrol: Shanghai McLean Biochemical Technology Co., Ltd; Hyaluronic acid (14,000) (HA-TLM 20–40): Huaxi Bio-technology Co., Ltd; Carboxymethylcellulose Sodium (CMC-Na): Shanghai Aladdin Biochemical Technology Co. Ltd; Tween 80: Shanghai Aladdin Biochemical Technology Co., Ltd; Poloxamer 188 (P188): Jiangsu Green Leaf Biotechnology Co., Ltd; Tepan Blue test solution: Beijing Solebao Technology Co: Self-made in the laboratory.

Methods

Preparation of resveratrol nanocrystals (Res-NC)

In this study, Res NC was prepared by media milling method. firstly, the magnetic rotor was added into a clean syringe bottle (20 mL), the stabilizer was weighed precisely in the syringe bottle, 1 mL of deionized water was added to dissolve it by ultrasonication, and then the weighed Res was weighed precisely to add into the syringe bottle to ultrasonically dispersed, and then the ZrO_2 with the diameter of 0.5 mm was added, and then the deionized water was added slowly by drops with the syringe to the syringe bottle until the horizontal surface diffused over the ZrO_2 interface of about 3 ~ 4 mm, sealed and then driven by a magnetic stirrer to grind ZrO_2 for several hours. After grinding, the nanosuspension was sucked into the EP tube with a syringe, and then 3 mL of deionized water was washed in the vial in five times, and the washing solution was added into the EP tube to obtain the Res NC, which was then put into the freeze-dryer to freeze-dry for 12 h to obtain the Res NC lyophilized powder. The optimal preparation process of Res NC was obtained by screening the type of stabilizer, the ratio of stabilizer to drug, the amount of ZrO_2 and the grinding time.

Screening of stabilizers The nanoscale particles have large surface energy, which requires the addition of suitable stabilizers to avoid secondary aggregation between particles through spatial site resistance and electrostatic repulsion. In this experiment, the following factors were fixed firstly: the dose of API (20 mg/mL), the amount of ZrO_2 (4 mL), the rotational speed of magnetic stirrer

(600 r/min), the milling time of 8 h, and the types of stabilizers (CMC-Na, PVP, SDS, Tween 80, and Poloxamer 888888888888888) were screened. The specific experimental steps were processed according to the operation of 2.2.1, and the particle size and dispersion coefficient were measured in a laser particle sizer after the preparation to determine the most suitable stabilizer type.

Screening of stabilizer to drug ratio The amount of stabilizer determines whether the surface of the particles can be completely wetted and thus the extent to which secondary aggregation of particles can be avoided. Therefore, the ratio of drug to stabilizer is equally important in influencing the particle size of the drug after milling. In this experiment, the following factors were fixed: the dose of API (20 mg/mL), the amount of ZrO_2 (4 mL), the grinding speed (600 r/min), the grinding time (8 h), the type of stabilizer SDS, and the ratio of stabilizer to drug was screened (the ratio of stabilizer to drug: 1:4, 1:2, 1:1, 2:1, 4:1). The specific experimental steps were processed according to the operation of 2.2.1, and the particle size and dispersion coefficient were measured in a laser particle sizer after the preparation to determine the most suitable ratio of stabilizer to drug.

Screening of ZrO_2 beads dosage The dosage of ZrO_2 determines the number of contact points with the API particles and has an effect on the particle size of the nanocrystals. In this experiment, the following factors were fixed: the dose of API (20 mg/mL), the ratio of stabilizer to drug of 1:1, the grinding speed (600 r/min), the grinding time (8 h), and the type of stabilizer SDS, and the dosage of ZrO_2 (2 mL, 4 mL, 6 mL, 8 mL, 10 mL) was screened. The specific experimental steps were processed according to the operation of 2.2.1, and the particle size and dispersion coefficient were measured in a laser particle sizer after the preparation to determine the most suitable amount of ZrO_2.

Screening of grinding time The grinding time has a great influence on the particle size and PDI of the particles, so it is necessary to investigate the grinding time. In this experiment, the following factors were fixed: the dose of API (20 mg/mL), the ratio of stabilizer to drug was 1:1, the amount of ZrO_2 (4 mL), the rotational speed of the magnetic stirrer (600 r/min), the type of stabilizer SDS, and the milling time (2 h, 4 h, 8 h, 12 h, and 24 h) was screened. The specific experimental steps were processed according to the operation of 2.2.1, and the particle size and dispersion coefficient were measured in a laser particle sizer after preparation to determine the most suitable grinding time.

Determination of Res NC solubility

The dialysis bag diffusion method was used to investigate Res API and Res NC for in vitro release experiments. Res API (the dispersion medium was deionized water containing 1% SDS), Res API + Res-NC mixed solution and Res-NC solution (all at 1 mg/mL) were prepared separately and 1 mL of each was taken in a dialysis bag (MW: 14,000 Da), which was placed in a centrifuge tube containing 20 mL of release medium (PBS solution containing 1% SDS, pH = 7.4), and finally, the tubes were transferred to a centrifuge tube with a rotational speed of 150 r/min, pH = 7.4, and a speed of 1mL. The dialysis bags were placed in centrifuge tubes containing 20 mL of release medium (PBS solution containing 1% SDS, pH = 7.4), and finally the centrifuge tubes were transferred to a shaker with a rotational speed of 150 r/min and a temperature of 37 ℃, and 1 mL of the samples were taken at 0.5, 1, 2, 4, 6, 8, 12, 24, 48, and 72 h after the release, and the isothermal and isocratic volume of the release medium was replenished. After the samples were filtered through a 0.22 μm membrane, the concentration of Res was determined by HPLC and the cumulative release was calculated. Calculation formula:

$$E_r\% = \frac{V_e\sum_{i=1}^{n-1}C_i + V_0C_n}{m_{drug}} \times 100\%$$

V_n: sampling volume; C_i: concentration of Res at the sampling (μg/mL); C_n: concentration of resveratrol at the nth sampling (μg/mL); V_0: volume of PBS release medium (mL); m_{drug}: mass of resveratrol weighed (μg).

Resveratrol nanocrystal cytotoxicity assay

Murine RAW264.7 macrophages were gifted by the School of Pharmacy, Yantai University. The cells were cultured in RPMI 1640 medium containing 10% FBS, penicillin (1%) and streptomycin (1%) at 37 °C in a humidified incubator with 5% CO_2.

RAW264.7 cells in logarithmic growth phase and in good condition were inoculated into 96-well plates with a cell density of 1×10^5/well, and cultured in a sterile cell culture incubator at 37℃ with 5% CO_2 for 24 h. After the cells were completely attached to the wall, the original medium was discarded, and different concentrations of Res-NC solutions prepared in advance were added to the

Table 1 Stabilizer screening experiments($n=3$)

Stabilizer type	Nanocrystal grain size/nm	PDI
CMC-Na	534.3 ± 2.78	0.407 ± 0.007
Poloxamer188	452.8 ± 3.65	0.303 ± 0.005
Tween 80	320.9 ± 1.45	0.398 ± 0.008
PVP	286.5 ± 1.37	0.324 ± 0.006
SDS	210.9 ± 0.64	0.301 ± 0.002

Table 2 Stabilizer to drug ratio screening experiments($n=3$)

Stabilizer-drug ratio	Nanocrystal grain size/nm	PDI
1: 5	568.8 ± 1.67	0.385 ± 0.007
1: 2	425.9 ± 2.54	0.243 ± 0.003
1: 1	375.9 ± 1.34	0.214 ± 0.008
2: 1	339.9 ± 0.38	0.244 ± 0.006
4: 1	434.0 ± 2.98	0.350 ± 0.005

corresponding wells, respectively. After 24 and 48 h of incubation, the medium containing different concentrations of Res-NC solution was discarded, washed three times with PBS, and then 20μL of MTT solution at a concentration of 5 mg/mL was added to each well, and incubated for 4 h, protected from light. after the incubation was completed, the MTT solution was discarded, and 100μL of DMSO was added to each well, and placed on a shaking table at 37℃ for 15 min, in order to fully dissolve the methanol at the bottom. crystals, and finally, the absorbance at 570 nm was detected by multifunctional enzyme marker and the cell viability was calculated.

Free radical scavenging capacity of Res NC by DPPH method

Upon addition of antioxidant to the DPPH solution, a decolorization reaction occurs and the change in absorbance can be used to determine the antioxidant capacity of the antioxidant compound. Different amounts of Res-NC were added to the DPPH solution and after the reaction of Res-NC as an antioxidant with the assay working solution, the absorbance was measured at 515 nm using an enzyme meter.

Preparation of microneedles

Preparation of Res-NC MNs

Precisely weigh 100 mg of HA in a centrifuge tube, add an appropriate amount of Res-NC solution, stir to fully dissolve the HA to a gel, and leave it overnight to make the bubbles disappear to obtain the Res-NC MNs matrix. The Res-NC MNs matrix was uniformly injected into a clean PDMS mold (30 × 30, H = 600 μm, L = 500 μm), and gently shaken to ensure the uniform thickness of the liquid in the mold. Subsequently, the molds were placed into a vacuum drying oven for evacuation for 1 h. After removal, the molds were dried at room temperature and demolded for subsequent experiments. The morphology of the Res-NC MNs was observed with a camera, an optical microscope and a scanning electron microscope, respectively, and photographs were taken to record the observations.

Res NC MNs performance testing

Skin puncture performance testing The prepared Res-NC MNs were cut into 10 × 10 arrays with a scalpel and set aside for skin-piercing experiments. SD rats were firstly dehairing and subsequently euthanized, and the treated abdominal skin was cut off with scissors and fixed. The Res-NC MNs were inserted vertically into the skin of the rats, pressed for 1 min and then stained, and the excess staining solution was removed with cotton balls, and the stained area was rinsed with 0.9% saline, and the number of stained pinholes was observed and recorded. At the same time, frozen sections of the microneedle-punctured skin were taken, and the pore structure left by the Res-NC MNs was observed under a light microscope.

Skin recovery performance test The dorsal layer of Res-NC MNs was held with tweezers and the dorsal layer of Res-NC MNs was adhered to the pre-prepared tape. The tape was placed on the abdomen of the depilated rats and pressed for 1 min to allow complete puncture of the skin cuticle. Skin conditions at the time of microneedle removal were recorded at 0 min, 10 min, 30 min, and 1 h, respectively.

Dissolution of the Res-NC MNs The prepared MNs were cut into 1 × 11 arrays with a scalpel, and the edges of the backing layer were clamped with tweezers and pierced into the skin of the treated mice, and pressed for 30 s, 60 s, and 120 s. The Res-NC MNs were removed from the skin at different time points, and pasted on slides, and the intradermal dissolution of the tips of the Res-NC MNs

Table 3 Screening experiments on the amount of ZrO_2 bead dosage($n=3$)

ZrO_2 beads dosage/mL	Nanocrystal grain size/nm	PDI
2	405.2 ± 6.65	0.362 ± 0.008
4	266.0 ± 1.43	0.215 ± 0.002
6	359.4 ± 0.21	0.244 ± 0.008
8	428.6 ± 1.89	0.322 ± 0.006
10	471.9 ± 4.76	0.473 ± 0.005

Table 4 Experimental data for grinding time screening($n=3$)

Grinding time/h	Nanocrystal grain size/nm	PDI
2	562.5 ± 5.93	0.207 ± 0.007
4	439.6 ± 4.87	0.204 ± 0.006
8	339.4 ± 5.65	0.287 ± 0.008
12	197.6 ± 4.73	0.173 ± 0.004
24	210.0 ± 4.42	0.224 ± 0.003

at different times was observed and photographed and recorded under an optical microscope.

In vivo pharmacodynamic studies

Male SD rats (SPF grade, 180 g ~ 200 g). The experimental procedures were performed in strict accordance with the relevant regulations of the Committee for the Management and Use of Laboratory Animals of Yantai University.

AIA arthritis modeling and grouping

The AIA model was established by subcutaneous injection of complete Freund's adjuvant (FCA) into the right hind foot of SD rats at 0.20 mL each. Saline was injected subcutaneously into the right hind foot of the control group as a blank control. The SD rats were equally divided into five groups, the control group, the AIA model group, the oral Res administration group, and the Res NC MNs administration group, with three rats in each group, The Res dose for each formulation group was 10 mg/kg, and the dosing cycle was once every two days, starting on the 11th day after modeling. The therapeutic effects of different preparations in rats for the treatment of rheumatoid arthritis were evaluated by evaluating the degree of swelling of the hind feet of the rats in the primary and secondary tests, as well as by staining H&E pathology sections of the hind feet of the rats, and by immunohistochemistry to observe anti-inflammatory effects. Finally, the safety

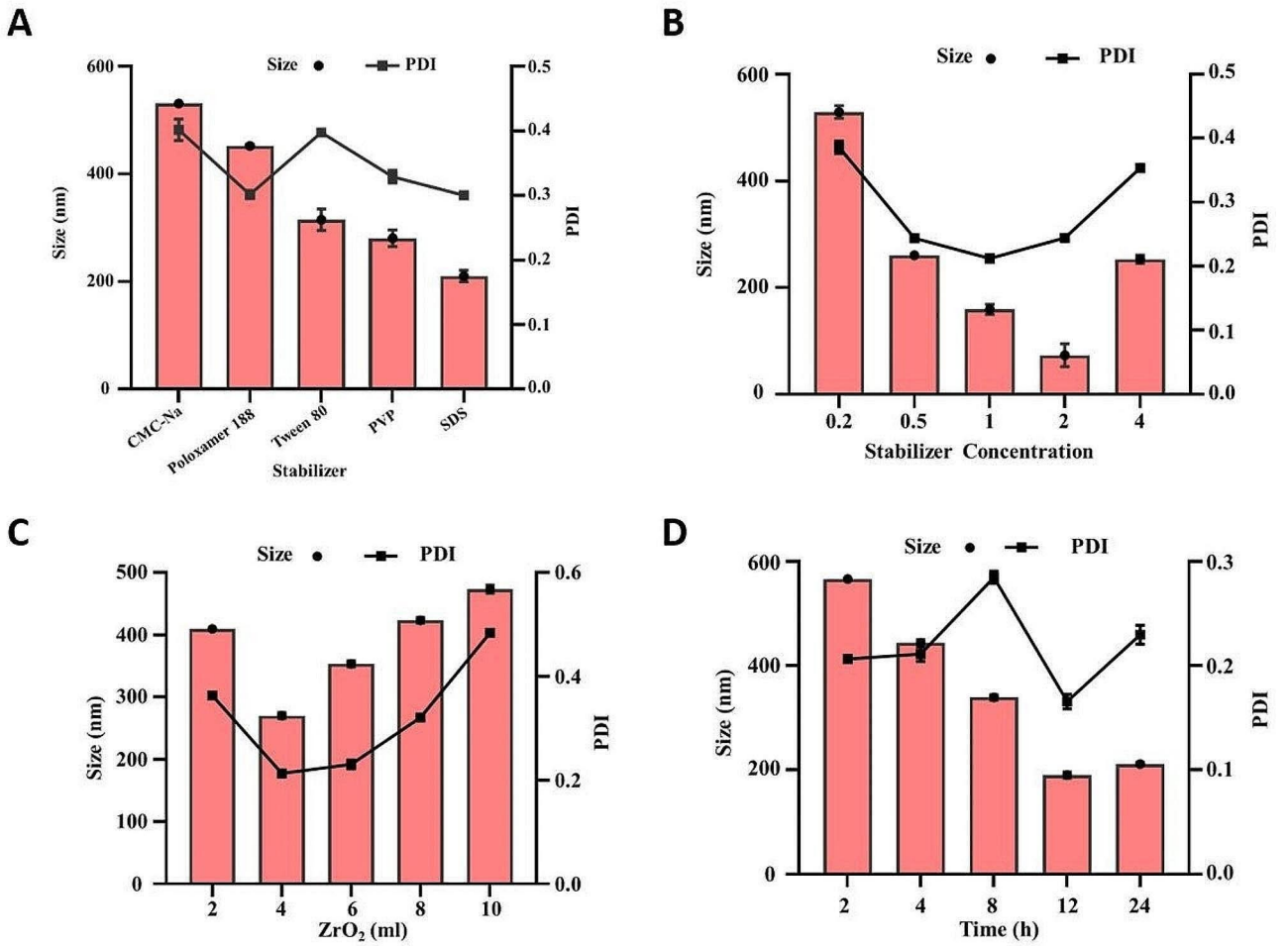

Fig. 1 Prescription screening for the preparation of resveratrol nanocrystals. **A**: Screening of stabilizer type **B**: Screening of stabilizer to drug ratio **C**: Screening of ZrO_2 beads dosage **D**: Screening of milling time. Data are expressed as mean ± SD ($n=3$)

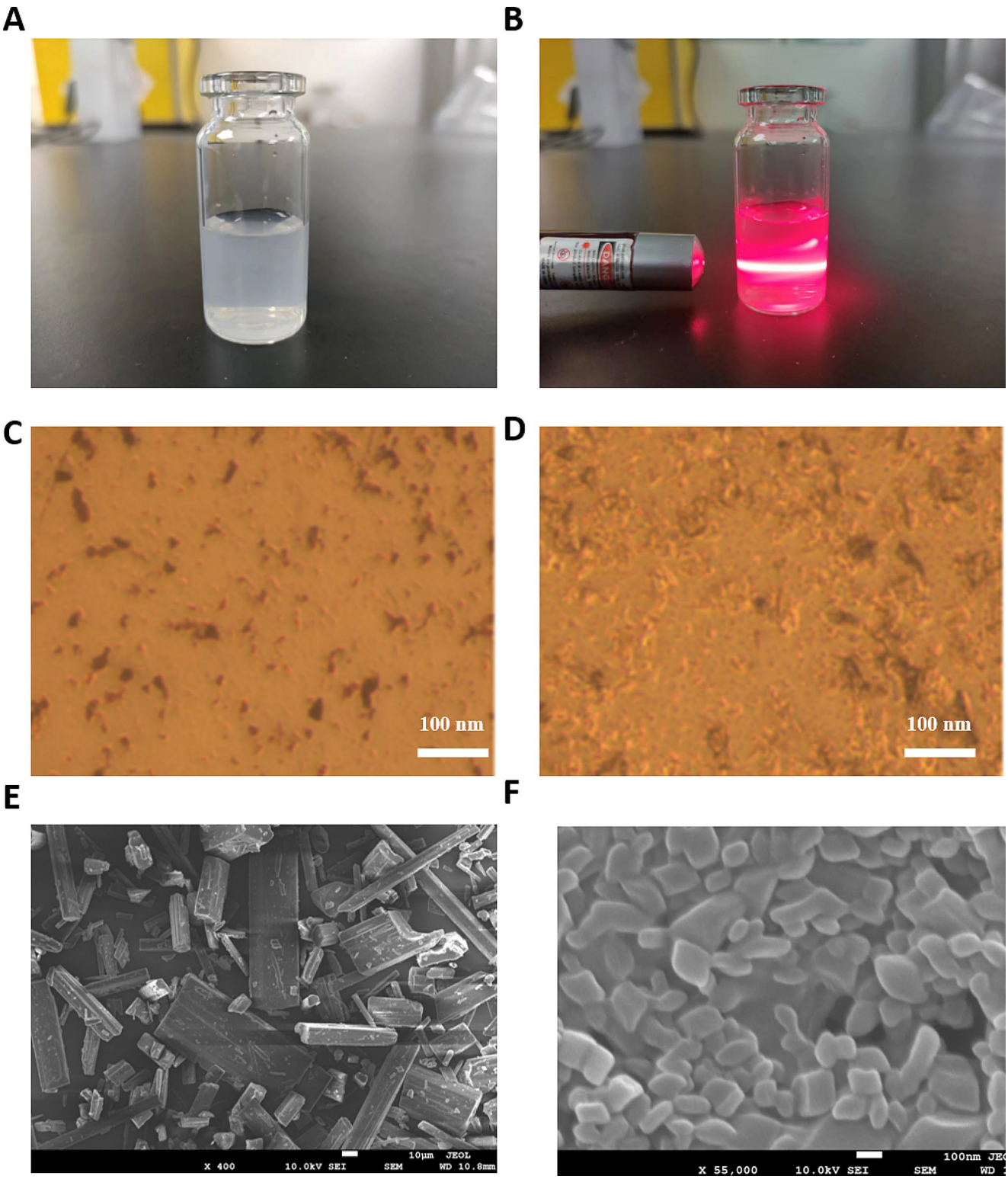

Fig. 2 **A**: Res-NC solution **B**: Res NC laser irradiation phenomenon **C**: Res API micro imaging **D**: Res-NC lyophilized particles micro imaging **E**: Res API SEM imaging **F**: Res-NC lyophilized particles SEM imaging

of the different preparations in vivo was judged by body weight changes and organ histopathological evaluation.

Measurement of joints swelling rate

In this experiment, the trend in the rate of swelling of

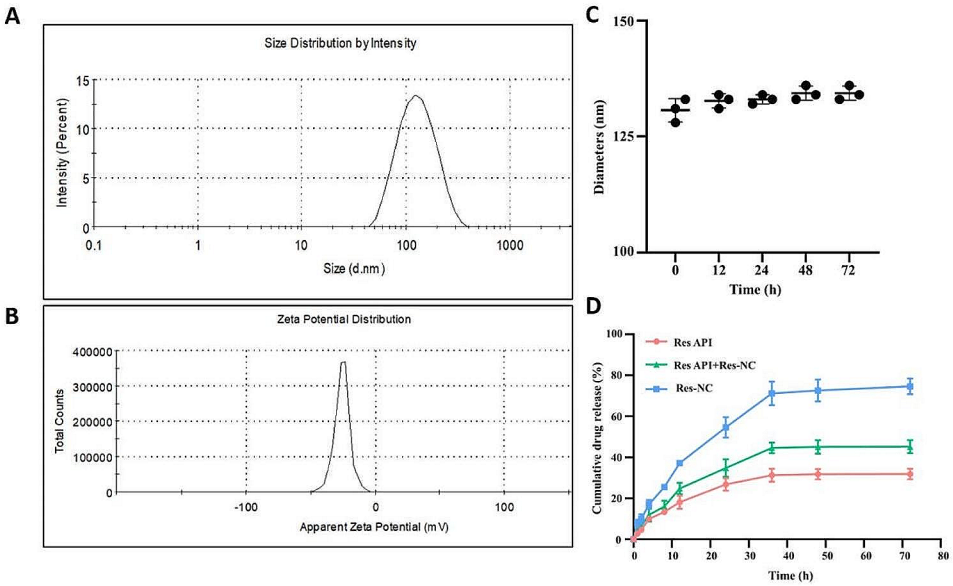

Fig. 3 **A**: Res-NC particle size **B**: Res-NC zeta potential C: Res-NC particle size stability test D: Res-NC external release. Data are expressed as mean ± SD ($n = 3$)

the primary measured joints after the start of modeling and the rate of swelling of the secondary measured joints, which differed in the time of the start of measurement, were counted. Significant swelling of the primary joints was seen on the third day after modeling, and the degree of swelling of the primary joints was measured by toe volumetry on days 3, 6, 9, 12, 15, 18, 21, 24, 27, and 30, respectively. The success of the modeling was demonstrated by swelling of the secondary joint on day 11, and the swelling of the secondary joint was measured by toe volumetry on days 12, 15, 18, 21, 24, 27, and 30 after modeling. The weight of each group was weighed at the same time as each toe volume measurement and the change in weight was recorded.

Histopathological studies of joints

After the last administration, the rats were anesthetized with 10% chloral hydrate, photographs of the hindfoot joint area were taken in each group, followed by cardiac perfusion, and the joint tissues were excised 2 cm out from the top and bottom of the ankle joints of the rats and immersed in paraformaldehyde solution for fixation, followed by decalcification, dehydration, paraffin embedding, filming and H&E staining. At the same time, the synovial tissue was removed and labeled with immunoproteins, and the brown area was the positive expression area. Pathologic sections were observed with a light microscope and photographed.

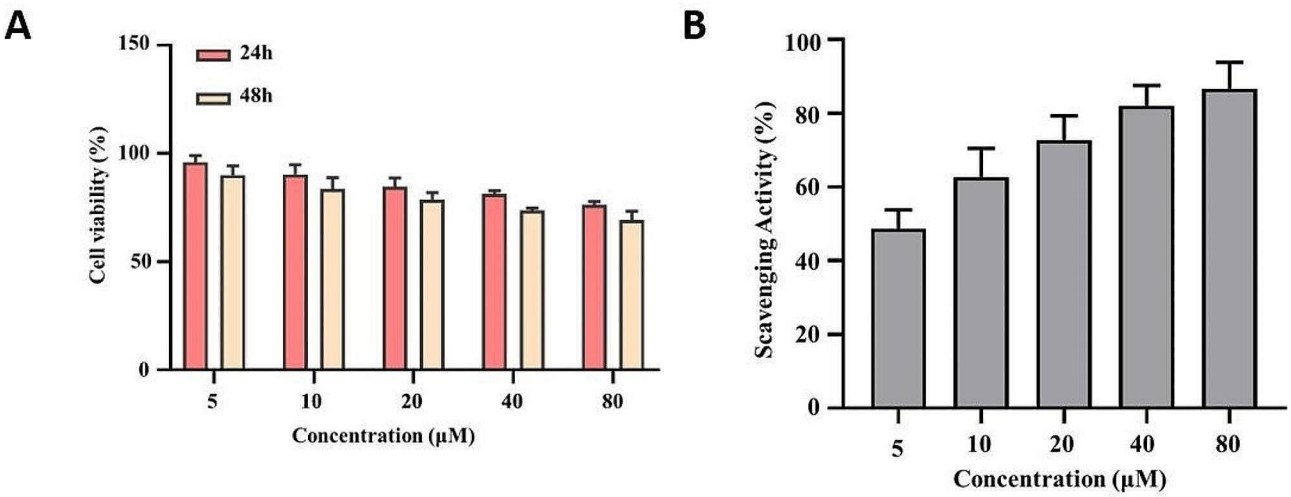

Fig. 4 **A**: Res-NC cytotoxicity assay **B**: Res-NC free radical scavenging capacity assay. Data are expressed as mean ± SD ($n = 3$)

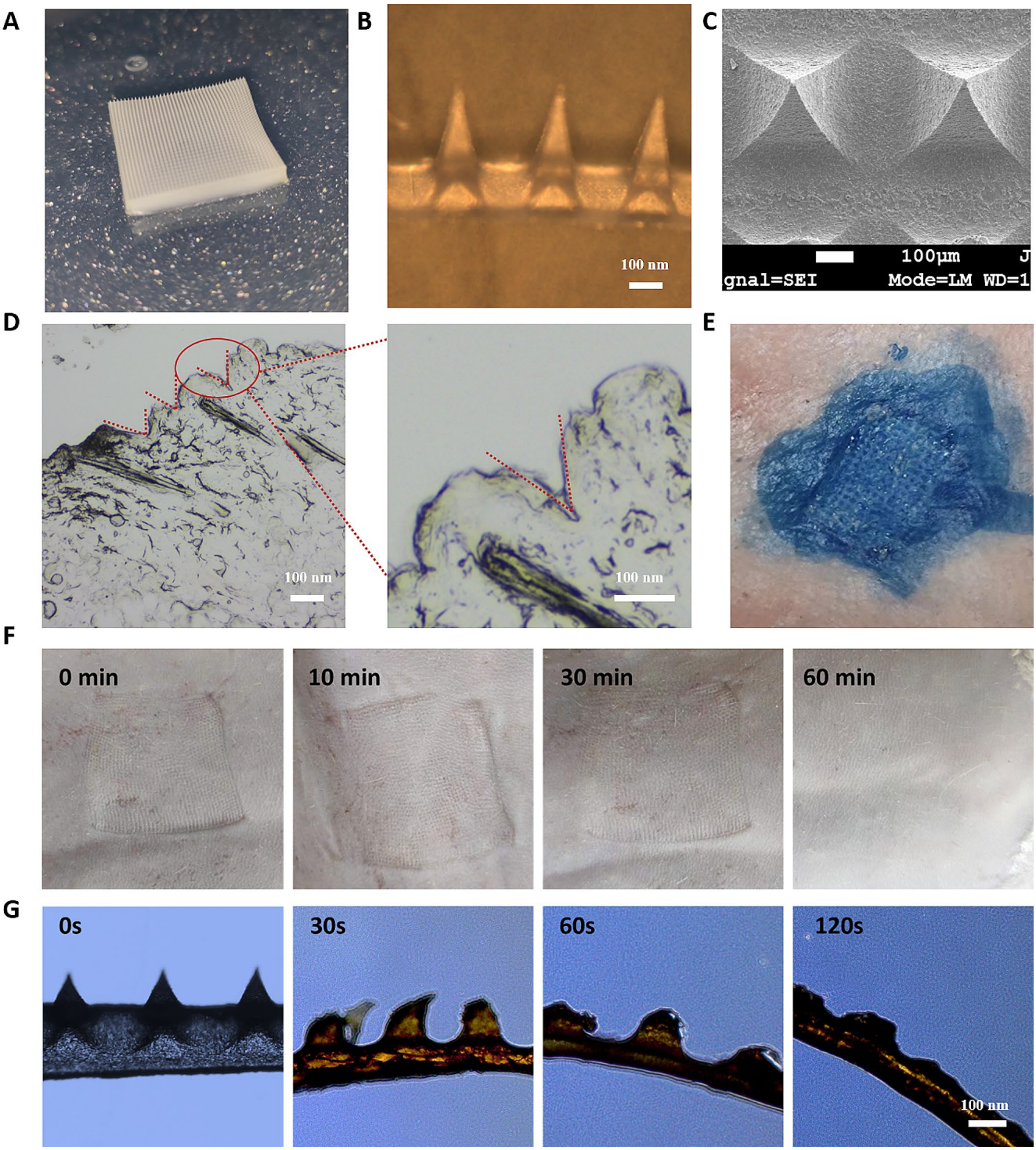

Fig. 5 Examination of the basic morphology of Res-NC MNs **A**: Res-NC MNs appearance and morphology **B**: Res NC MNs optical microscope imaging **C**: Res-NC MNs SEM imaging **D**: Res NC MNs skin puncture performance tissue examination. **E**: Res-NC MNs Skin Piercing Study **F**: Res NC MNs solubility experiment **G**: Res NC MNs skin penetration performance

In vivo safety evaluation

In this experiment, the in vivo safety was assessed by monitoring the changes in body weight and H&E staining pathology of major organs (heart, liver, spleen, lungs and kidneys) of rats at the end of drug administration. The skin of the rats was also observed for redness and swelling after microneedle administration.

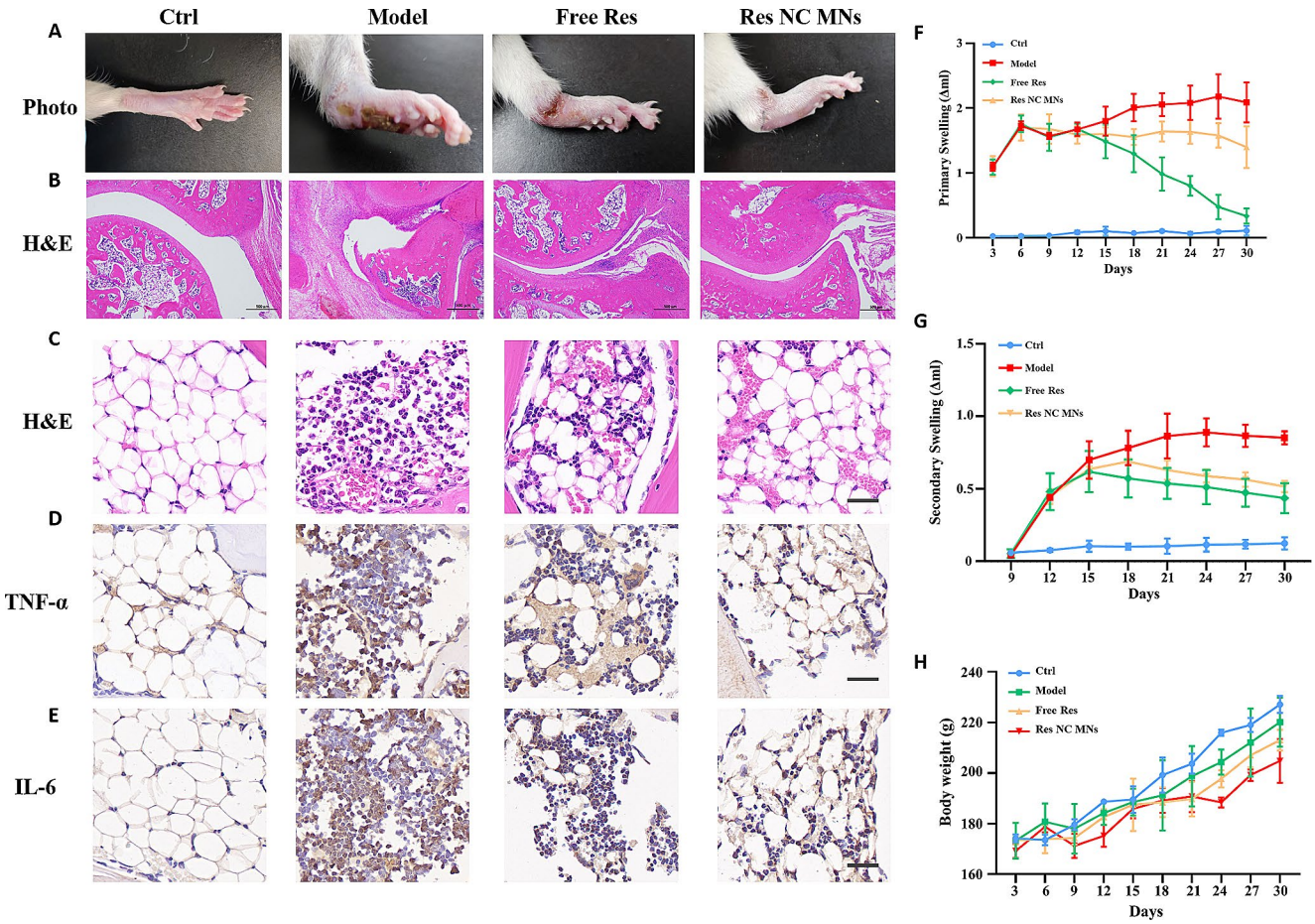

Fig. 6 **A**: Photographs of AIA model **B**: H&E staining of cartilage tissue **C**: H&E staining of synovial tissue **D**: TNF-α immunohistochemistry **E**: IL-6 immunohistochemistry **F**: Swelling rate of the primary side **G**: Swelling rate of the secondary side **H**: Changes in body weight of the rats. (scare bar = 200 nm)

Results and discussion

Screening of stabilizer type

As shown in Table 1, five types of stabilizers, CMC-Na, PVP, SDS, Tween 80, and Poloxamer 188, were added to prepare Res-NC under the conditions of controlled variables, and the results showed that when the stabilizer was SDS, the particle size of Res-NC was the smallest, about 210 nm or so, and the PDI was smaller, which was enough to show that among the above types of stabilizers, SDS was the most suitable stabilizer for the preparation of This is enough to show that among the above types of stabilizers, SDS is the most suitable stabilizer for the preparation of Res-NC, so SDS was chosen as the stabilizer for the preparation of Res-NC in this study.

Screening of the ratio of stabilizer to drug

As shown in Table 2, under the condition of controlling variables, the ratio of stabilizer to drug was set as 1:5, 1:2, 1:1, 2:1, 4:1 in this experiment, respectively, under different ratios for the preparation of Res-NC. The results showed that when the ratio of drug to stabilizer was 1:1 and 2:1, the particle size of the prepared Res-NC was small, which was around 350 nm. In order to improve the drug content of Res-NC, we finally chose a smaller amount of SDS for the preparation of Res-NC, i.e., the ratio of drug to stabilizer was 1:1.

Screening of ZrO_2 bead dosage

As shown in Table 3, in the limited space, under the condition of controlling variables, in a certain range, the more ZrO_2 content the more adequate grinding, so the particle size of Res-NC decreases with the increase of ZrO_2 dosage, but the excessive dosage of ZrO_2 also leads to the larger

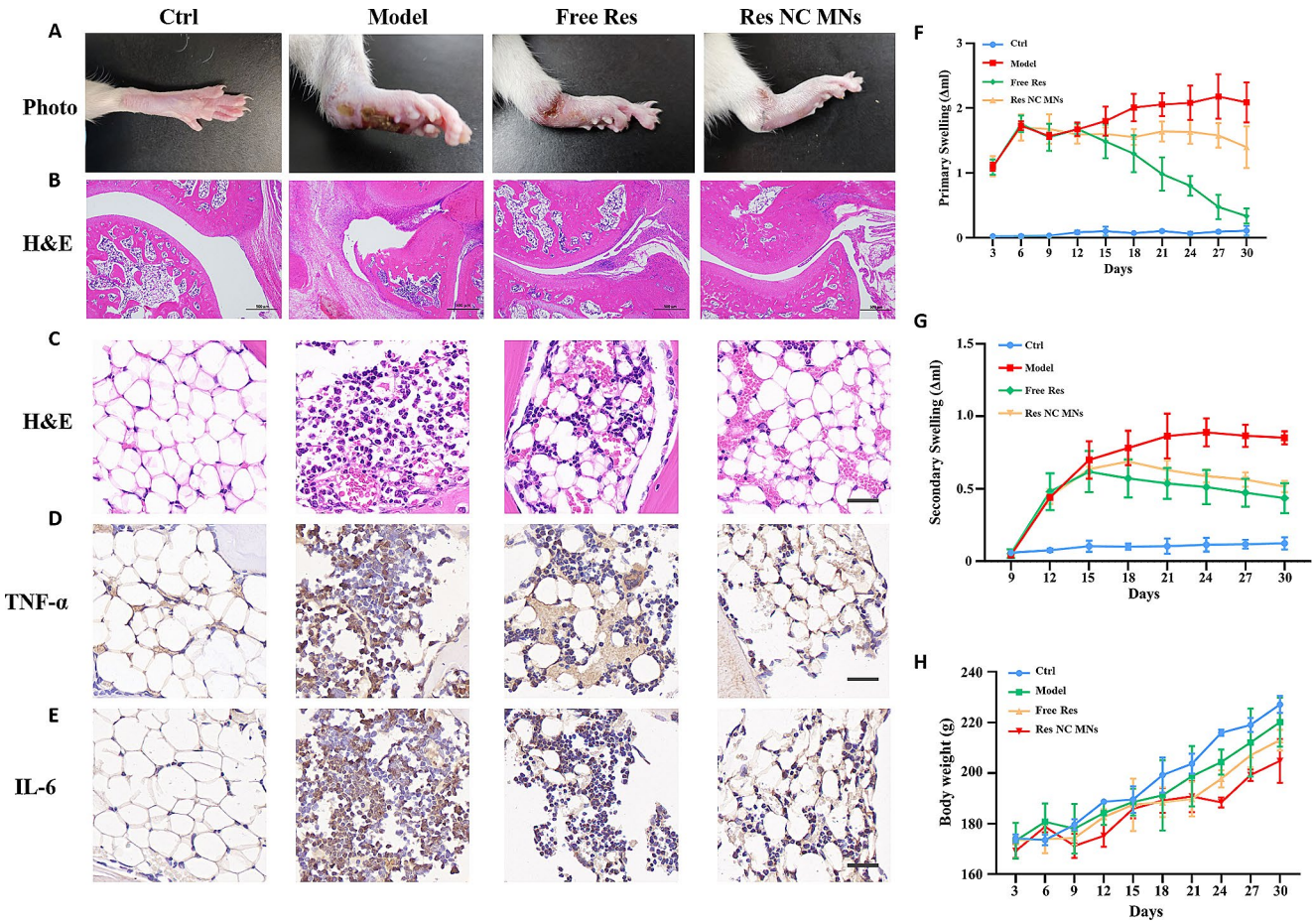

Fig. 7 **A**: H&E staining of major organs **B**: Pictures of skin irritation response in rats before and after drug administration. (scare bar = 200 μm)

particle size and poorer dispersion, and the dosage of ZrO_2 is crucial for the particle size of Res-NC. The experimental results showed that when the dosage of ZrO_2 was 4 mL, the prepared Res NC had smaller particle size and better dispersion. Therefore, 4 mL of ZrO_2 needs to be added when preparing Res-NC.

Screening of grinding time

As shown in Table 4, under the condition of controlling variables, 2, 4, 8, 12, and 24 h were milled respectively, and the results showed that, within a certain range, the longer the milling time, the smaller the particle size and the better the dispersibility of the Res-NC obtained, and at the milling time of 12 h, the particle size of the Res-NC was about 180 nm, and the PDI was about 0.160, which was in line with the expectation, so we chose the preparation of the Res-NC at a grinding time of 12 h.

In summary, this experimental sieve finally screened out the optimal preparation process for the preparation of Res-NC as follows: 20 mg of SDS was weighed precisely in a 10 mL vial, 2 mL of deionized water was added, and ultrasonication was performed for 2 min to make it fully dissolved. Subsequently, 20 mg of resveratrol was weighed precisely, added with 2 mL of deionized water, dispersed by ultrasonication for 1 min, and mixed with the above SDS solution, then added with 4 mL of ZrO_2, and placed on a magnetic stirrer and milled at room temperature for 12 h. Res-NC with small particle size and homogeneous and stable was obtained, and the changes of the particle size of Res-NC and the PDI under the conditions of different variables were shown in Fig. 1. The variation of Res-NC particle size and PDI under different variable conditions is shown in Fig. 1.

Examination of resveratrol nanocrystals morphology

The Res-NC solution prepared using the optimal prescription was colloidal, uniformly dispersed and without obvious precipitation (Fig. 2.A). Irradiation with a laser pointer produced a bright pathway, i.e., the Tyndall effect (Fig. 2. B), which further indicated that the Res-NC solution was homogeneous and without precipitation, and it could be

preliminarily judged that the Res-NC preparation was successful. The Res API and the Res-NC showed different morphologies under the optical microscope (Fig. 2.C,D), and Res NC was more homogeneous as compared with the Res API. Under the scanning electron microscope, it can be observed that Res-NC has smaller particle size and more uniform morphology compared with Res API, indicating that Res-NC was successfully prepared (Fig. 2. E, F).

Res-NC particle size and potential distribution

The prepared Res-NC was placed in a laser particle sizer to check its particle size and potential. The results showed that the particle size of Res-NC was about 130 nm and PDI 0.20 (Fig. 3.A). The results show that the Res-NC prepared in this experiment has uniform particle size, good dispersion, and is stable in solution without aggregation, and the potential distribution of Res-NC is around −32 mV (Fig. 3.B). The particle size stability of Res-NC was evaluated, and it was found that the particle size change of Res-NC was small within 72 h (Fig. 3.C), with no obvious aggregation and precipitation phenomenon, which was in line with the requirements of the late experiments. From the in vitro release results, it can be seen that the release of Res API was about 30% within 72 h, the mixed solution of Res API and Res-NC, the release reached about 45% within 72 h, and Res-NC was about 80% within 72 h (Fig. 3.D), which indicates that preparing Res into nanocrystals can effectively reduce the particle size of Res-NC and significantly improve the Res solubility.

Cytotoxicity and free radical scavenging capacity studies of Res-NC

We tested Res-NC for cytotoxicity and antioxidant capacity. The results showed that the concentration of Res-NC up to 80μM still achieved about 70% cell survival within 48 h (Fig. 4A), indicating that Res-NC had no obvious cytotoxicity and had good safety and biocompatibility to be used in subsequent experiments. Free radical scavenging assay showed that Res-NC had strong ROS scavenging ability (Fig. 4B).

Examination of the morphology of Res-NC MNs

After the Res-NC MNs were demolded, the backing layer was transparent, the needle body was full and pyramidal with no broken needles, and the backing layer was intact with uniform thickness and no air bubbles, so it was initially judged that the preparation of MNs was successful (Fig. 5A). Under the optical microscope, the Res-NC MNs were in the shape of a full pyramid, consistent with the visual morphology, the needle body and the backing layer were connected tightly, the thickness of the backing layer was uniform, and there were no air bubbles and voids (Fig. 5B). Under the scanning electron microscope, the Res-NC MNs were structurally complete and uniformly arranged, with no needle tip breakage, indicating that the Res-NC MNs were successfully prepared (Fig. 5C). Res-NC MNs had a certain mechanical strength to puncture the skin stratum corneum, and Res-NC MNs left obvious pinhole-like structures after piercing the skin (Fig. 5D). Staining of the Res-NC MNs after piercing into the skin revealed that all of the Res-NC MNs were pierced into the skin (Fig. 5E), further indicating that our prepared Res-NC MNs had a high molding rate and a certain mechanical strength. After piercing the skin, it could restore the skin condition in a relatively short time without causing irreversible damage (Fig. 5F), and the dissolution speed was fast and basically completely dissolved within 120 s, indicating that Res-NC MNs could release the drug in time to achieve a certain therapeutic effect (Fig. 5G).

In vivo pharmacodynamic evaluation

As shown in Fig. 6, the joint swelling rate of the AIA model group was significantly increased compared with that of the control group (Fig. 6A). H&E staining pathology showed that the AIA model group displayed a large number of neutrophils and lymphocytes infiltration and a severe inflammatory reaction compared with the control group. And compared with the AIA model group, the free Res administration group and the Res-NC MNs administration group all reduced the inflammatory response to different degrees, with the Res-NC MNs having the best effect in inhibiting the inflammatory response (Fig. 6B). H&E staining of the synovial membrane showed that the synovial membrane structure was infiltrated by inflammatory cells and the typical honeycomb structure was disrupted in the AIA model group, and the situation improved after the administration of each preparation group, with the improvement being more obvious in the Res-NC MNs group (Fig. 6C). The TNF-α and IL-6 expression levels were significantly higher in the Model group compared to the control group. Compared with the Model group, the TNF-α and IL-6 protein contents of synovial and cartilage tissues in each treatment group decreased to different degrees, with the most obvious decrease in protein contents in the Res-NC MNs group, indicating that the Res-NC MNs treatment was able to effectively alleviate inflammation at the joint site (Fig. 6D and E). When the administration of Res-NC MNs began on the 12th day, there was a trend of reduction in the rate of joint swelling in all groups, among which the Res-NC MNs administration group showed a more obvious trend of reduction, which indicated that the Res-NC MNs administration group

was able to significantly inhibit the joint swelling of rats with AIA-type arthritis (Fig. 6F and G). The body weights of rats in all groups increased to different degrees, with the most obvious increase in the control group, while the body weights of rats in the AIA model group and other administration groups increased slowly, which might be related to the inflammatory response (Fig. 6H).

In vivo safety evaluation

As shown in the Fig. 7, there was no significant histological damage in the H&E-stained pathograms of the major organs (heart, liver, spleen, lungs and kidneys) of the different dosing groups in SD rats compared to the control group; therefore, Res-NC MNs had no significant systemic toxicity in SD rats (Fig. 7A). At the end of the administration, no significant erythema was observed in the Res NC MNs group compared to the other groups. (Fig. 7B)

Conclusion

In this study, a transdermal drug delivery system based on soluble microneedles prepared from HA encapsulating Res-NC was constructed. The optimal preparation process of Res-NC was determined by screening the type of stabilizer, the ratio of stabilizer to drug, the amount of grinding beads, and the grinding time. The prepared Res-NC were also examined for morphology, particle size, potential and drug release, and the experimental data showed that the nanocrystals prepared by the optimal process had good stability, solubility properties and no obvious cytotoxicity. The prepared Res-NC MNs was examined for appearance, skin puncture, skin recovery, and skin dissolution, and the experimental results showed that the prepared Res-NC MNs had good morphology, good skin puncture rate and did not affect the skin recovery. It is feasible to use HA to prepare MNs carrying Res-NC to improve their bioavailability. It was found that a transdermal drug delivery system mediated by soluble MNs improved patient compliance and prolonged the duration of drug action in vivo, while mitigating the inflammatory effects and inhibiting the progression of RA by suppressing excess ROS during RA development. Provides a new research idea for the treatment of RA.

Author contributions Ningning Diao: Contributed to the conception of the study, experimented. Yan Liu: Revised the manuscript. Wenxin Wang and Min Cao: Visualization, Data curation. Xiaowei Liu and Weili Yang: Visualization, Data curation. Tianying Sun and Huijie Pei: Performed the data analyses and wrote the manuscript. Chunjing Guo: Helped perform the analysis with constructive discussions. Daquan Chen: Conceptualization, Data curation, Funding acquisition, Methodology, Project administration, Resources, Supervision, Validation, Writing-review & editing.

Funding All authors acknowledge financial support from Natural Science Foundation of Shandong Province (No. ZR2019ZD24, ZR2019YQ30); Taishan Scholar Foundation of Shandong Province (No. qnts20161035); Graduate Innovation Foundation of Yantai University, GIFYTU.

Data availability The datasets generated during and/or analysed during the current study are available from the corresponding author on reasonable request.
Neither the entire paper nor any part of its content has been published or has been accepted elsewhere. It is not being submitted to any other journal. Hope this study can be suitable for the journal.

Declarations

Ethics approval and consent to participate All experiments were conducted by the ARRIVE Guidelines and were approved by the Animal Ethics Committee of Yantai University (Ethical Annotation License Number: YTU20220923). Male Sprague-Dawley rats (180 ~ 200 g) were purchased from Jinan Pengyue Experimental Animal Breeding Co., Ltd. (Shandong, China). All animals have free access to food and water and are housed at a temperature of 22 ± 1°C, relative humidity of 50 ± 1%, and a light/dark cycle of 12/12 h. Before administration, the rats were anesthetized with intra-peritoneal injection of anesthetics (80 mg/kg ketamine and 4.5 mg/kg xylazine) while monitoring body temperature with a feedback-conditioned heating pad. Rats were euthanized by intraperitoneal injection of excessive pentobarbital sodium. The study does not involve human subjects.

Consent for publication All authors have read and agreed to the published version of the manuscript.

Competing interest The authors declare no competing interests.

References

1. Alivernini S, Firestein GS, McInnes IB. The pathogenesis of rheumatoid arthritis. Immunity. 2022;55:2255–70.
2. Zaiss MM, Joyce Wu H-J, Mauro D, Schett G, Ciccia F. The gut–joint axis in rheumatoid arthritis. Nat Rev Rheumatol. 2021;17:224–37.
3. Scherer HU, Häupl T, Burmester GR. The etiology of rheumatoid arthritis. J Autoimmun. 2020;110:102400.
4. Adawi M, Watad A, Bragazzi NL, Amital H, Saaida G, Sirchan R, Blum A. Endothelial function in rheumatoid arthritis. QJM: Int J Med. 2018;111:243–7.
5. Brock J, Basu N, Schlachetzki JCM, Schett G, McInnes IB, Cavanagh J. Immune mechanisms of depression in rheumatoid arthritis. Nat Rev Rheumatol. 2023;19:790–804.
6. van Delft MA, Huizinga TW. An overview of autoantibodies in rheumatoid arthritis. J Autoimmun. 2020;110:102392.
7. Weyand CM, Goronzy JJ. The immunology of rheumatoid arthritis. Nat Immunol. 2021;22:10–8.
8. McInnes IB, Schett G. Pathogenetic insights from the treatment of rheumatoid arthritis. Lancet. 2017;389:2328–37.
9. Wang J, Zeng J, Liu Z, Zhou Q, Wang X, Zhao F, Zhang Y, Wang J, Liu M, Du R. Promising strategies for Transdermal Delivery of Arthritis drugs. Microneedle Systems; 2022. p. 14.
10. Chen K, Zhao Y, Zhao W, Mao X, Li D, Wang Y, Shang S, Zhang H. Lubricating Microneedles System with Multistage Sustained Drug Delivery for the Treatment of Osteoarthritis, Small, (2024) e2307281.

11. Wang Q, Yang X, Gu X, Wei F, Cao W, Zheng L, Li Y, Ma T, Wu C, Wang Q. Celecoxib Nanocrystal-loaded dissolving microneedles with highly efficient for osteoarthritis treatment. Int J Pharm. 2022;625:122108.
12. Cao J, Su J, An M, Yang Y, Zhang Y, Zuo J, Zhang N, Zhao Y. Novel DEK-Targeting Aptamer delivered by a Hydrogel Microneedle attenuates Collagen-Induced Arthritis. Mol Pharm. 2021;18:305–16.
13. Yu K, Yu X, Cao S, Wang Y, Zhai Y, Yang F, Yang X, Lu Y, Wu C, Xu Y. Layered dissolving microneedles as a need-based delivery system to simultaneously alleviate skin and joint lesions in psoriatic arthritis. Acta Pharm Sinica B. 2021;11:505–19.
14. Rajendran K, Pahal S, Badnikar K, Nayak MM, Subramanyam DN, Vemula PK, Krishnan UM. Methotrexate delivering microneedle patches for improved therapeutic efficacy in treatment of rheumatoid arthritis. Int J Pharm. 2023;642:123184.
15. Xie J, Zhu X, Wang M, Liu C, Ling G, Zhang P. Dissolving microneedle-mediated transdermal delivery of flurbiprofen axetil-loaded pH-responsive liposomes for arthritis treatment. Chem Eng J. 2024;482:148840.
16. Du G, He P, Zhao J, He C, Jiang M, Zhang Z, Zhang Z, Sun X. Polymeric microneedle-mediated transdermal delivery of melittin for rheumatoid arthritis treatment. J Controlled Release. 2021;336:537–48.
17. Oh WY, Shahidi F. Lipophilization of Resveratrol and effects on antioxidant activities. J Agric Food Chem. 2017;65:8617–25.
18. Pang Q, Wang C, Li B, Zhang S, Li J, Gu S, Shi X. Resveratrol-loaded copolymer nanoparticles with anti-neurological impairment, antioxidant and anti-inflammatory activities against cerebral ischemia–reperfusion injury. Arab J Chem. 2024;17:105393.
19. Hu LF, Lan HR, Li XM, Jin KT. A Systematic Review of the Potential Chemoprotective Effects of Resveratrol on Doxorubicin-Induced Cardiotoxicity: Focus on the Antioxidant, Antiapoptotic, and Anti-Inflammatory Activities, Oxid Med Cell Longev, 2021 (2021) 2951697.
20. Li W, Yuan H, Liu Y, Wang B, Xu X, Xu X, Hussain D, Ma L, Chen D. Current analytical strategies for the determination of resveratrol in foods. Food Chem. 2024;431:137182.
21. Zhang X, Li Z, Gao J, Wang Z, Gao X, Liu N, Li M, Zhang H, Zheng A. Preparation of nanocrystals for Insoluble drugs by top-down nanotechnology with improved solubility and bioavailability. Molecules; 2020. p. 25.
22. Zheng Y, Wang Y, Xia M, Gao Y, Zhang L, Song Y, Zhang C. The combination of nanotechnology and traditional Chinese medicine (TCM) inspires the modernization of TCM: review on nanotechnology in TCM-based drug delivery systems. Drug Deliv Transl Res. 2022;12:1306–25.
23. Colombo M, Staufenbiel S, Rühl E, Bodmeier R. In situ determination of the saturation solubility of nanocrystals of poorly soluble drugs for dermal application. Int J Pharm. 2017;521:156–66.
24. Pang Z, Zhang J, Cao W, Kong X, Peng X. Partitioning surface ligands on nanocrystals for maximal solubility. Nat Commun. 2019;10:2454.